HIV-1 Nef mobilizes lipid rafts in macrophages through a pathway that competes with ABCA1-dependent cholesterol efflux[S]

Huanhuan L. Cui,[1,*] Angela Grant,[1,2,†] Nigora Mukhamedova,[*] Tatiana Pushkarsky,[†] Lucas Jennelle,[†] Larisa Dubrovsky,[†] Katharina Gaus,[§] Michael L. Fitzgerald,[**] Dmitri Sviridov,[3,*] and Michael Bukrinsky[†]

Baker Heart and Diabetes Institute,* Melbourne, VIC, Australia; Department of Microbiology, Immunology and Tropical Medicine,† George Washington University, Washington, DC; Centre for Vascular Research,§ University of New South Wales, Sydney, NSW, Australia; and Lipid Metabolism Unit,** Massachusetts General Hospital, Boston, MA

Abstract HIV infection, through the actions of viral accessory protein Nef, impairs activity of cholesterol transporter ABCA1, inhibiting cholesterol efflux from macrophages and elevating the risk of atherosclerosis. Nef also induces lipid raft formation. In this study, we demonstrate that these activities are tightly linked and affect macrophage function and HIV replication. Nef stimulated lipid raft formation in macrophage cell line RAW 264.7, and lipid rafts were also mobilized in HIV-1-infected human monocyte-derived macrophages. Nef-mediated transfer of cholesterol to lipid rafts competed with the ABCA1-dependent pathway of cholesterol efflux, and pharmacological inhibition of ABCA1 functionality or suppression of ABCA1 expression by RNAi increased Nef-dependent delivery of cholesterol to lipid rafts. Nef reduced cell-surface accessibility of ABCA1 and induced ABCA1 catabolism via the lysosomal pathway. Despite increasing the abundance of lipid rafts, expression of Nef impaired phagocytic functions of macrophages. The infectivity of the virus produced in natural target cells of HIV-1 negatively correlated with the level of ABCA1. These findings demonstrate that Nef-dependent inhibition of ABCA1 is an essential component of the viral replication strategy and underscore the role of ABCA1 as an innate anti-HIV factor.—Cui, H. L., A. Grant, N. Mukhamedova, T. Pushkarsky, L. Jennelle, L. Dubrovsky, K. Gaus, M. L. Fitzgerald, D. Sviridov, and M. Bukrinsky. **HIV-1 Nef mobilizes lipid rafts in macrophages through a pathway that competes with ABCA1-dependent cholesterol efflux. *J. Lipid Res.* 2012.** 53: **696–708.**

Supplementary key words cholesterol metabolism • cholesterol trafficking • ATP binding cassette transporter A1 • human immunodeficiency virus

Impairment of cholesterol metabolism plays a key role in pathogenesis of many disorders, most importantly cardiovascular and neurodegenerative diseases. Many infectious agents, from prions to parasites, affect cholesterol metabolism of the host. Microorganisms modify host cholesterol metabolism for two main reasons: to satisfy their own requirements for cholesterol at different stages of their life cycle, and to weaken the immune response of the host. These modifications may cause "unintended" consequences, triggering development of diseases that are not directly related to infection. This situation is exemplified by the increased risk of atherosclerosis coincident with HIV infection. Targeting cholesterol metabolism for antimicrobial intervention, while at the same time correcting metabolic consequences of the infection, is a tempting possibility limited by the lack of knowledge about mechanisms of interaction between microorganisms and pathways of cholesterol metabolism in host cells.

This work was supported by the National Institutes of Health Grants HL-093818, HL-101274, and AI-078743 (M.B. and D.S.); by National Health and Medical Research Council of Australia Grant 526615 (D.S. and M.B.); in part by the Victorian Government Operational Infrastructure Support (OIS) program; and in part by the District of Columbia Developmental Center for AIDS Research (DC D-CFAR), a National Institutes of Health-funded program (Grant 1P30AI-087714-01). The contents are solely the responsibility of the authors and do not necessarily represent the official views of the National Institutes of Health. D.S. is a fellow of the National Health and Medical Research Council of Australia (Grant 586607).

Manuscript received 29 November 2011 and in revised form 15 January 2012.

Published, JLR Papers in Press, January 19, 2012
DOI 10.1194/jlr.M023119

Abbreviations: AcLDL, acetylated LDL; CT-B, cholera toxin subunit B; BLT, blocking lipid transfer; GP, generalized polarization; LAMP-1, lysosome-associated membrane protein-1; LPS, lipopolysaccharide; LXR, liver X receptor; MDM, monocyte-derived macrophage; PBL, peripheral blood leukocyte; PDM, product of the differences from the mean.

[1] H. L. Cui and A. Grant contributed equally to this work.

[2] Present address of A. Grant: Harvard School of Public Health AIDS Initiative, Department of Immunology and Infectious Diseases, Harvard School of Public Health, Boston, MA.

[3] To whom correspondence should be addressed.
e-mail: Dmitri.Sviridov@bakeridi.edu.au

[S] The online version of this article (available at http://www.jlr.org) contains supplementary data in the form of one figure.

It has been established that HIV infection interferes with cholesterol metabolism of host cells, particularly macrophages, elevating the risk of atherosclerosis; however, the mechanisms of this connection are not completely understood (for review, see Ref. 1). We have reported that HIV replication is associated with impairment of both local and systemic elements of the reverse cholesterol transport pathway (2, 3), which plays a key role in maintaining cellular cholesterol homeostasis. HIV, via the viral accessory protein Nef, inhibits activity of the ATP binding cassette transporter A1 (ABCA1), an integral transmembrane lipid transporter (4), and impairs cholesterol efflux from macrophages, causing accumulation of cholesterol in these cells and their transformation into foam cells, a hallmark of atherosclerosis (3). Furthermore, extracellular Nef secreted by HIV-infected cells can inhibit cholesterol efflux from uninfected cells and cause impairment of systemic reverse cholesterol transport (5). On the other hand, stimulation of cholesterol efflux through activation of ABCA1 suppresses HIV-1 infection (6). These findings suggest that interaction between Nef and ABCA1 may be a key to both viral replication and impairment of cellular lipid metabolism. The cellular mechanisms of Nef interaction with ABCA1 and how this interaction translates into physiological effects related to HIV replication and macrophage functions remain unknown. Understanding the mechanisms of Nef effects on ABCA1 may provide important information for elucidating novel pathways responsible for regulation of ABCA1 abundance and functionality. The involvement of these pathways may not be limited to HIV infection, as they may represent a physiological regulation of cellular cholesterol metabolism exploited by HIV and possibly by other infections.

Nef exerts pleiotropic effects during viral infection, and although Nef expression is not strictly essential for viral replication in vitro, it significantly enhances infectivity of nascent virions (7). One mechanism by which Nef controls viral infectivity is through increasing cholesterol content of lipid rafts (8). Nef induces a number of genes involved in cholesterol synthesis (8, 9) and can facilitate cholesterol delivery to lipid rafts (8, 10). This activity is consistent with membrane localization of Nef due to myristoylation (8, 11, 12); nonmyristoylated Nef did not affect lipid rafts (8). Lipid rafts are the preferential sites of HIV-1 assembly and budding, and cholesterol content of lipid rafts determines the cholesterol content of virions, which is critical for virion infectivity. Cholesterol depletion of HIV-infected cells reduces infectivity of released virions, which was shown to correlate with the amount of virion-associated cholesterol and the activity of Nef (6, 13). In addition, depletion of cellular cholesterol, which reduces the abundance of rafts, also reduces HIV-1 particle production (6, 10). Therefore, primary cholesterol-related activity of Nef may be to increase the abundance of lipid rafts, thus stimulating production and infectivity of nascent HIV virions. How this capacity of Nef relates to cellular pathways involved in maintaining cholesterol homeostasis and, specifically, why and how Nef inhibits ABCA1 remains unclear. It is also unknown what role, if any, inhibition of ABCA1 plays in the effect of Nef on lipid rafts. In this study, we investigated the association among Nef, ABCA1, and lipid rafts. We hypothesized that HIV Nef is responsible for either inhibition or subversion of the ABCA1-dependent pathway of cholesterol trafficking, redirecting the flow of intracellular cholesterol from cholesterol efflux to formation of lipid rafts, and that this phenomenon is essential for HIV infectivity. Our results demonstrate that inhibition of ABCA1 is critical for Nef-dependent modulation of lipid rafts and illustrate consequences of this modulation for the cell and the virus.

MATERIALS AND METHODS

Cells

N7 mouse macrophage cell line was obtained from the Centre for AIDS Reagents (NIBSC). These cells were derived from the RAW 264.7 mouse macrophage cell line and are stably transfected to express a low level of HIV-1 viral protein Nef that is inducible by treatment with cadmium chloride ($CdCl_2$) (14). HeLa-ABCA1 cells stably expressing GFP-tagged ABCA1 (15, 16) were a kind gift of Dr. A. Remaley. Peripheral blood leukocytes and monocyte-derived macrophages were isolated and maintained as described previously (3).

Antibodies for Western blot analysis

The monoclonal antibody against ABCA1 was from Novus Biologicals, anti-JR-CSF Nef monoclonal antibody was from NIH AIDS Research and Reference Reagent Program; antibodies to Notch 3, Integrin 5β, and GAPDH were from Santa Cruz Biotechnology; and anti-β-actin monoclonal antibody was from Sigma. Horseradish peroxidase cholera toxin subunit B conjugate for detection of GM1 and transferrin receptor antibodies were from Invitrogen.

Isolation of apoA-I

High-density lipoprotein ($1.083 < d < 1.21$ g/l) was isolated by sequential centrifugation in KBr solutions, delipidated, and apoA-I was purified by gel filtration chromatography as previously described (17).

siRNA experiments

Cells were treated with TO-901317 (0.5 μM) for 18 h, and then transfected with ABCA1- or Nef-specific siRNA or scrambled siRNA (control) using Lipofectamine 2000™ (Invitrogen). ABCA1 siRNA and scrambled siRNA were from Ambion. Nef siRNA was custom designed and manufactured by Invitrogen.

Analysis of HIV-1 infectivity

Monocyte-derived macrophages were infected with HIV-1 ADA and maintained for 10 days until infection reached the plateau (5×10^3 cpm/ml of RT activity). Cells were transfected with ABCA1-targeting or control siRNA twice with a 24 h interval, washed, and cultured for two days after the second transfection. Virus was collected from the supernatant, concentrated, adjusted according to p24 content, and used to infect indicator TZM-bl cells (18). At 48 h after infection, luciferase activity was measured on PerkinElmer luminescence counter.

Lipid raft cholesterol content analysis

To assess the transfer of cholesterol to lipid rafts, we used three approaches. The first approach utilized a selective binding of

cholera toxin subunit B (CT-B) to GM1, a marker of rafts. The cells were treated with 0.5 μM of liver X receptor (LXR) agonist TO-901317 and treated or not with 10 μM $CdCl_2$ for 24 h, washed with PBS, detached by trypsin, washed again, and incubated for 1 h at 4°C in serum-containing medium with FITC-CT-B conjugate (Invitrogen) (final concentration 0.5 μg/ml). Cells were then fixed with 5% formaldehyde and analyzed by flow cytometry.

The second approach relied on increased susceptibility for oxidation of cholesterol in cholesterol-rich domains by extracellular cholesterol oxidase as was described previously (19). Briefly, RAW 264.7 or N7 cells were treated with 0.5 μM TO-901317, treated or not with 10 μM $CdCl_2$, and simultaneously labeled for 24 h with [^{3}H]cholesterol (Amersham-GE, specific radioactivity 1.81 TBq/mmol; final radioactivity 75 kBq/ml) at 37°C. Final amount of labeled cholesterol in the cells was similar for all cells and conditions. Cells were then treated with cholesterol oxidase for 3 h at 4°C. Lipids were extracted and samples together with lipid standards were fractionated by TLC (19).

The third approach analyzed physicochemical properties of the cell plasma membrane by Laurdan 2-photon microscopy. RAW 264.7 or N7 cells were plated in 24 well plates at 0.1×10^6 cells/well. The cells were treated with 0.5 μM TO-901317 for 24 h and treated or not with 10 μM $CdCl_2$ for 24 h. Cells were labeled with 5 μM Laurdan (6-dodecanoyl-2-dimethylaminonaphtalene; Invitrogen) for 30 min at 37°C, washed three times with PBS, and fixed in 4% paraformaldehyde at room temperature for 20 min. Images were obtained using TCS SP5 2-photon microscope (Leica) equipped with photomultiplier tubes and acquisition software (Leica). Laurdan dye was excited at 800 nm with a 2-photon laser (Mai-Tai HP; Spectra-Physics), and emission intensities were recorded simultaneously in the ranges of 400–460 nm and 470–530 nm. Laurdan dye intensity images for each pixel were converted into generalized polarization (GP) images using custom-made algorithm. The GP is defined as: $GP = (I_{(400-460)} - I_{(470-530)} / (I_{(400-460)} + I_{(470-530)})$, where I is the emission intensity. GP distributions were obtained from the histograms of the GP images, normalized (sum = 100), and fitted to Gaussian distributions using a nonlinear fitting algorithm.

Cell fractionation

To isolate the membrane fraction, RAW 264.7 and N7 cells were washed with cold PBS, resuspended in 5 mM Tris buffer, incubated for 30 min at 4°C, and freeze-thawed twice. Debris was removed by low-speed centrifugation, and supernatant was subjected to centrifugation at 100,000 *g* for 1 h at 4°C. The pellet was resuspended in buffer containing 50 mM Tris, protease and phosphatase inhibitors cocktail (Roche), 2 mM β-mercaptoethanol, and 1% Triton X-100.

Lipid rafts from membrane fraction of RAW 264.7 and N7 cells labeled with [^{3}H]cholesterol were isolated by centrifugation in OptiPrep density gradient medium (Sigma) according to manufacturer's instructions. Fractions were analyzed by Western blot developed with anti-GM1 and anti-ABCA1 antibodies.

Isolation of intracellular and membrane fractions of HeLa-ABCA1 cells was performed using commercially available Pierce Cell Surface Protein Isolation Kit (Thermo Scientific) following manufacturer's protocol. Equal amounts of protein were loaded on the purification column. Fractionation was assessed via Western blot for membrane and cytosolic protein markers.

Biotinylation of ABCA1

Cells were activated with TO-901317 (0.5 μM), treated with $CdCl_2$ (10 μM) for 24 h, and incubated for 30 min at 4°C in PBS with Sulfo-NHS-SS-Biotin (Pierce) (final concentration 0.5 mg/ml). Cells were scraped into PBS containing protease and phosphatase inhibitor cocktail (Roche) and homogenized. Large debris removed by low speed centrifugation, and the membrane fraction was isolated as described above. Equal amounts of protein were mixed with UltraLink Plus immobilized streptavidin gel and incubated for 18 h at 4°C. After extensive washing, beads were mixed with loading buffer containing 50 mM DTT, heated at 37°C for 30 min, and then the gel was pelleted. The pelleted gel was separated by SDS-PAGE and blotted with antibodies to ABCA1 and GAPDH.

Confocal microscopy

For imaging, HeLa-ABCA1-GFP cells were grown on 35 mm glass-bottom cell culture dishes. GM1 staining was performed using Alexa Fluor 555/CT-B conjugate (Invitrogen). Lysosome labeling was performed using Organelle Lights™ specifically labeling lysosome-associated membrane protein-1 (LAMP-1). Twenty four hours prior to imaging, cells were transduced with the Organelle Lights Lysosomes-RFP reagent according to the manufacturer protocol (Invitrogen). Images were captured with a Zeiss LSM 510 Confocal Microscope equipped with integrated on-stage incubator chamber. The chamber provides constant temperature at 37°C and is supplied with humidified 5% CO_2. Two-channel confocal time series were captured at pixel resolution of 0.175 μm; image frames measured 512 × 512 pixels. Emission filtering was achieved by inserting on the backward light path high-pass 545 and 490 beam splitters in addition to a high-pass 505 filter. Images were taken by sequential line acquisition.

Quantitative colocalization was assessed using Volocity software (PerkinElmer). For colocalization, the images were first subjected to intensity threshold to eliminate the dark current registered at the image, followed by extracting the product of the differences from the mean (PDM). Positive PDM was determined for a single cell, in which pixel intensities of GFP and RFP vary synchronously and more positive PDM indicates a stronger degree of colocalization. We used the positive PDM as indicator for colocalizing pixels, as by definition, these pixels represent higher than the main pixel value (over threshold) for both channels and reduce the probability of including adjacent structures in the colocalization outcome. This protocol was applied to 10 cells per sample.

Cholesterol efflux

Cholesterol efflux was measured as described previously (20). Briefly, cells were incubated in serum-containing medium supplemented with [^{3}H]cholesterol (75 kBq/ml) for 48 h. Cells were then washed with PBS and incubated for 4 h in serum-free medium containing LXR agonist TO-901317. Apolipoprotein A-I was then added to the final concentration of 20 μg/ml. Aliquots of medium and cells were counted. The efflux was calculated as a proportion of radioactivity moved from medium to cells (minus efflux to medium without acceptors).

Cholesteryl ester biosynthesis

Cells were incubated for 18 h in serum-containing medium in the presence of 50 μg/ml of acetylated LDL (AcLDL). Cholesteryl ester biosynthesis was then assessed by incorporation of [^{14}C]oleic acid into cholesteryl esters over 2 h as described previously (3).

MTT assay

One hundred microliters of 3-(4,5-dimethylthiazol-2-yl)-2, 5-diphenyltetrazolium bromide (MTT) was added per 500 μl cell culture media, and cultures were incubated at 37°C for 3 to 4 h. The MTT/media mixture was removed, and 200 μl of an isopropanol/HCl mixture (500 ml isopropanol, 1.667 ml 12 M HCl) was used to dissolve cell pellets. The resulting supernatant was plated into 96-well plates and read in an ELISA reader at 570 nm.

Phagocytosis assay

RAW 264.7 and N7 cells were activated with LXR agonist TO-901317 (0.5 μM) and, where indicated, treated with $CdCl_2$ (10 μM) for 24 h. Phagocytosis was assessed using Phagocytosis Assay (Invitrogen) according to the manufacturer's instructions. For induced phagocytosis, cells were preconditioned by incubation for 18 h at 37°C with 1 μg/ml of lipopolysaccharide (LPS).

Endocytosis assay

RAW 264.7 and N7 cells were washed extensively with PBS, incubated for 1 h at 4°C (binding) or 37°C (internalization + binding) in serum-containing medium with FITC-CT-B conjugate (Invitrogen) (final concentration 0.5 μg/ml), and then scraped and analyzed by flow cytometry. Binding data is reported as mean fluorescence intensity (MFI) of cells maintained at 4°C.

Statistics

Unless indicated otherwise, the figures show the results of a representative experiment out of 2–4 identical experiments. Statistical analysis was performed using one-way ANOVA. Unless indicated otherwise, means ± SEM of quadruplicate determinations are presented.

RESULTS

In this study, we used mouse macrophage cell line N7, which is derived from RAW 264.7 cells and is stably transfected with HIV-1 Nef under Cd-activated promoter (14). This cell line was used because it is the only available cell line stably transfected with Nef under control of a regulated promoter and parent RAW 264.7 cells were previously used to study the effects of Nef (3). Activation of N7 cells with $CdCl_2$ led to a time-dependent elevation of the abundance of Nef, which leveled off after 24 h (**Fig. 1A**). However, low-level expression of Nef was observed in N7 cells not activated with $CdCl_2$, necessitating comparison of N7 cells with parent RAW 264.7 macrophages. To provide an additional control in these circumstances, we also tested three anti-Nef siRNAs at two concentrations. All siRNAs achieved over 70% reduction of Nef expression in N7 cells (Fig. 1B). In the subsequent experiments, we used $siRNA^{Nef}$#3 at concentration 20 nM.

To confirm the effect of Nef on cholesterol homeostasis in this model, we assessed cholesteryl ester biosynthesis, a surrogate measure of cholesterol accumulation, in these cells. Consistent with our previous findings in HIV-infected human macrophages (3), incorporation of [^{14}C]oleic acid into cholesteryl esters in N7 cells after loading with cholesterol by incubation with AcLDL was 50% higher than in RAW 264.7 cells (Fig. 1C). Knockdown of Nef expression in N7 cells with Nef siRNA brought cholesteryl ester biosynthesis in these cells to the level observed in RAW 264.7 cells, whereas transfection with control siRNA had no effect (Fig. 1C), showing that the observed effects were mediated by Nef and were not due to clonal variation between RAW 264.7 and N7 cell lines. For subsequent experiments, we compared N7 cells directly with RAW 264.7 cells.

Nef stimulates formation of lipid rafts

There is no commonly accepted approach to evaluate the amount of cholesterol in rafts and/or abundance of rafts; therefore, we used three independent methods to assess the effect of Nef on the abundance of lipid rafts. First, we used flow cytometry to assess binding to cells of cholera toxin subunit B, which binds specifically to the accepted marker of rafts, GM1. Results of these experiments are presented in **Fig. 2A**. Binding of CT-B to N7 cells expressing Nef increased 2-fold compared with the parent RAW 264.7 cells, and increased further upon stimulation of Nef expression by $CdCl_2$. Although $CdCl_2$ slightly decreased binding of CT-B to RAW 264.7 cells, the difference was not statistically significant. Both Nef-targeted and control siRNAs reduced CT-B binding, but the specifically targeted siRNA reduced binding to the level observed in RAW 264.7 cells, whereas CT-B binding to N7 cells treated

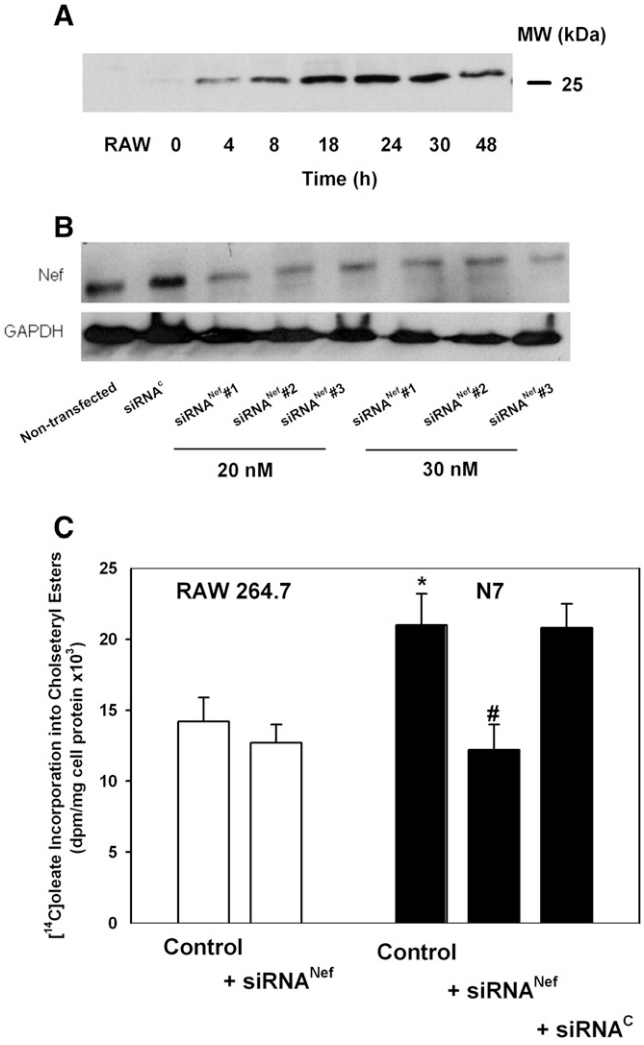

Fig. 1. Analysis of cholesteryl ester biosynthesis in RAW 264.7 and N7 cells. A: Nef expression in N7 cells. N7 cells were incubated for the indicated periods of time with $CdCl_2$ (10 μMol/l), and the abundance of Nef in total cell lysate was analyzed by Western blot. Left lane: lysate of RAW 264.7 cells. B: The effect of transfection of N7 cells with siRNA on the abundance of Nef. $siRNA^C$, control (scrambled) siRNA; $siRNA^{Nef}$, siRNA to Nef. C: Cholesteryl ester biosynthesis assessed as described in *Materials and Methods*. Both N7 and RAW 264.7 cells were treated with $CdCl_2$. Mean ± SEM of quadruplicate determinations. $^*P < 0.05$ (versus RAW 264.7 cells); $^{\#}P < 0.01$ (versus untransfected N7 cells).

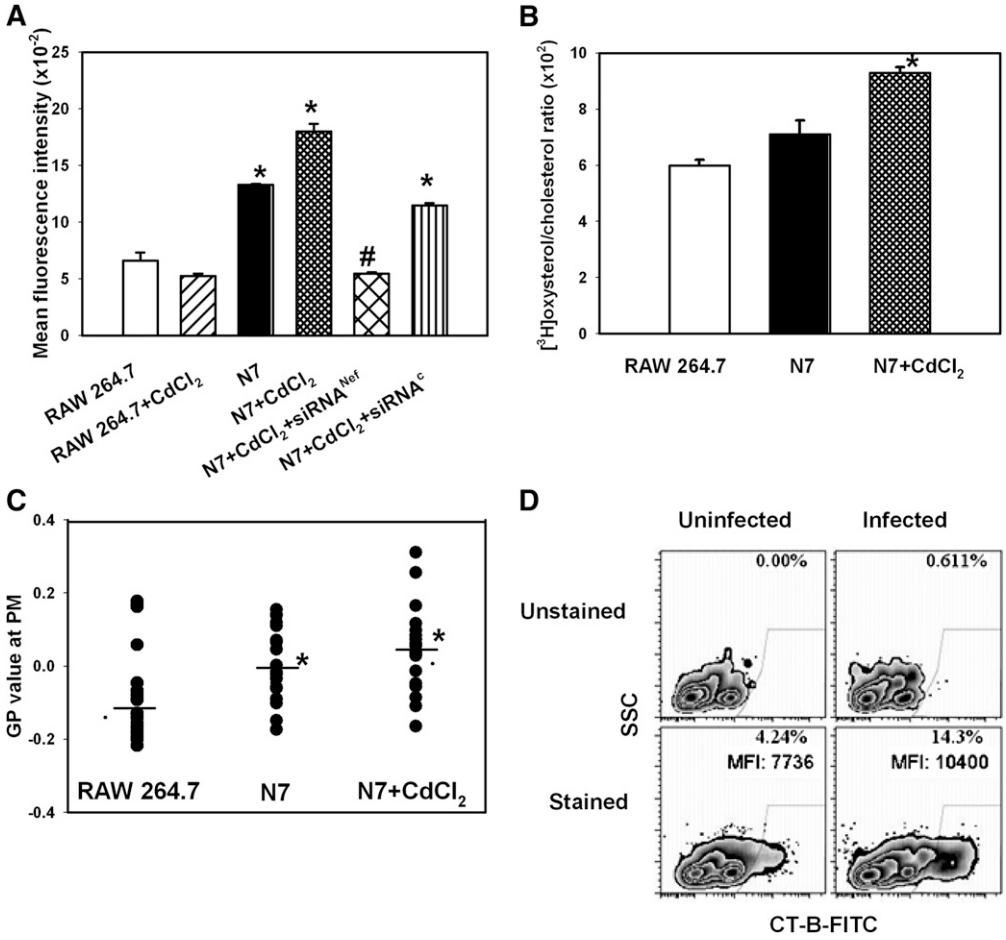

Fig. 2. Nef induces transport of cholesterol to lipid rafts. A: RAW 264.7 cells, N7 cells, and N7 cells activated with $CdCl_2$ were treated with cholera toxin B subunit (0.5 μg/ml); binding of CT-B to GM1 (a marker of rafts) was analyzed by flow cytometry. Results are presented as mean fluorescence intensity ± SEM of quadruplicate determinations. $^{*}P < 0.05$ (versus RAW 264.7 cells); $^{\#}P < 0.01$ (versus N7 cells). B: RAW 264.7 cells, N7 cells, and N7 cells activated with $CdCl_2$ were labeled with [^{3}H]cholesterol and treated with cholesterol oxidaze for 3 h on ice as described in *Materials and Methods*. Lipids were extracted and separated using TLC. Ratio of [^{3}H]oxysterol to [^{3}H]cholesterol is an indication of susceptibility of plasma membrane cholesterol to oxidation by extracellular cholesterol oxidase reflecting proportion of cholesterol in cholesterol-rich domains. Mean ± SEM of quadruplicate determinations. $^{*}P < 0.05$ (versus RAW 264.7 cells). C: RAW 264.7 cells, N7 cells, and N7 cells activated with $CdCl_2$ were stained with Laurdan dye (5 μM). GP value at the plasma membrane was analyzed in 20 images using 2-photon microscopy as described in *Materials and Methods*. $^{*}P < 0.05$ (versus RAW 264.7 cells). D: Monocyte-derived macrophages were infected or not with HIV-1 ADA and 14 days post infection were treated with FITC-conjugated CT-B at 4°C. Results are presented in a contour plot.

with siRNA^C was still significantly higher than binding to RAW cells (Fig. 2A).

Second, we used a biochemical approach assessing the susceptibility of plasma membrane cholesterol to oxidation by external cholesterol oxidase. Cholesterol accessible to the external enzyme has been suggested to be located in cholesterol-rich domains of the plasma membrane exposed to the cell surface, including caveolae (19) and lipid rafts (22). [RAW 264.7 cells and presumably N7 cells derived from RAW 264.7 cells do not have caveolae (21).] Results of these experiments are presented in Fig. 2B and show that Nef increased the proportion of cholesterol accessible to oxidation relative to total cholesterol.

Third, we measured membrane fluidity by analyzing Laurdan fluorescence recorded by a 2-photon microscopy (23, 24). The lipophilic dye Laurdan aligns itself parallel with the hydrophobic tails of the phospholipids in membranes and undergoes a shift in its peak emission wavelength from approximately 500 nm in fluid membranes to approximately 440 nm in ordered membranes due to partial penetration of water molecules into more fluid membranes (23). A normalized ratio of the two emission regions, calculated as the general polarization, provides a relative measure of polarity that can be equated to membrane order (24). Analysis of RAW 264.7 and N7 cells using this approach demonstrated that Nef expression increased the GP value (Fig. 2C), indicating an increase in membrane order, which is the biophysical hallmark of lipid rafts. Thus, although each raft detection method individually may not be unequivocal, data from each of the

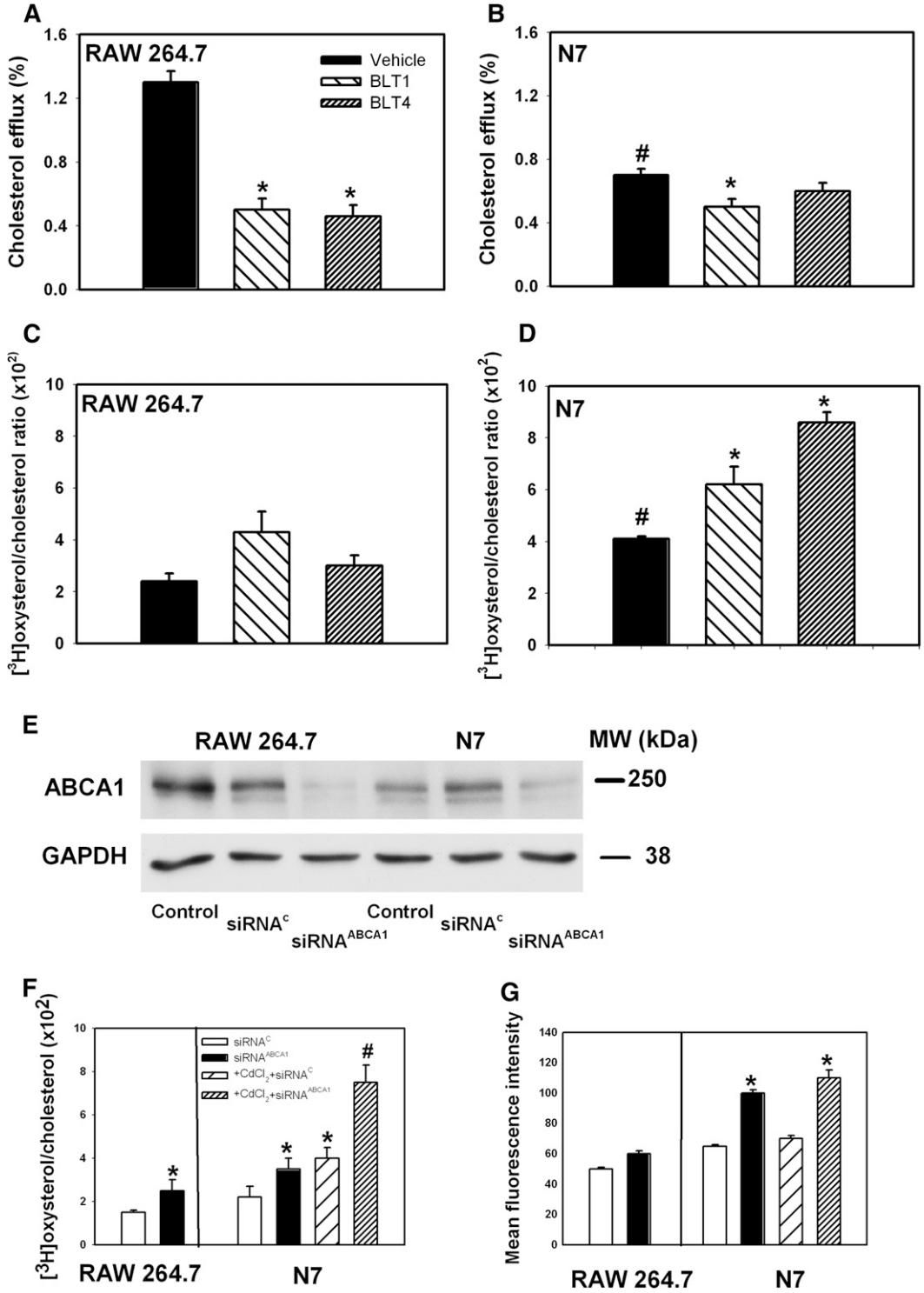

Fig. 3. Effect of ABCA1-trafficking inhibitors and ABCA1 knockdown on raft abundance. A–D: The effect of ABCA1-dependent trafficking inhibitors on cholesterol efflux and raft abundance. RAW 264.7 (A, C) or N7 (B, D) cells were labeled with [^{3}H]cholesterol, treated with a $CdCl_2$, and treated for 4 h with one of the BLT compounds (final concentration 10 μM for BLT-1 and 80 μM for BLT-4) or a vehicle. Cells were then washed and incubated with apoA-I (20 μg/ml) for 2 h, and cholesterol efflux was measured as described in *Materials and Methods* (A, B). Alternatively, cells were treated with cholesterol oxidase for 3 h on ice, and oxidation of plasma membrane cholesterol was assessed as described in *Materials and Methods* (C, D). Mean ± SEM of quadruplicate determinations are presented. A: $^*P < 0.05$ (versus vehicle). B: $^\#P < 0.01$ (versus RAW 264.7 cells treated with vehicle), $^*P < 0.05$ (versus N7 cells treated with vehicle). C: No significant differences between groups. D: $^\#P < 0.01$ (versus RAW 264.7 cells treated with vehicle), $^*P < 0.01$ (versus N7 cells treated under identical conditions). E–G: RAW 264.7 or N7 cells were treated with $CdCl_2$, labeled with [^{3}H]cholesterol, and either mock-transfected or transfected with ABCA1 siRNA (siRNA^{ABCA1}) or a control siRNA (siRNA^C) as described in *Materials and Methods*. E: Western blot showing ABCA1 abundance in cell lysate of

three methods support the conclusion that the presence of Nef increased the abundance of lipid rafts.

We further confirmed this finding using HIV-infected monocytes. Consistent with the findings in N7 cells, the percentage of cells with measurable CT-B binding increased from 4.2% to 14.3% when uninfected cells were compared with HIV-infected monocyte-derived macrophages (Fig. 2D), indicating that HIV-1 infection increases the abundance of lipid rafts in natural infection and validating N7 cells as a model for analysis of Nef effects in macrophages.

Inhibition of ABCA1 stimulates Nef-dependent formation of rafts

Given that Nef inhibits ABCA1-dependent cholesterol efflux while increasing the abundance of cholesterol in rafts, we investigated whether these two cholesterol-trafficking pathways (Nef-dependent and ABCA1-dependent) are connected. One possibility was that Nef "hijacks" ABCA1 and uses the ABCA1-dependent pathway to transfer cholesterol to rafts, instead of transferring it to an extracellular acceptor. Alternatively, Nef may compete with ABCA1 for cholesterol. To distinguish between these two possibilities, we inhibited ABCA1-dependent cholesterol trafficking and investigated the effect of this inhibition on Nef-dependent trafficking of cholesterol to rafts. We expected that if ABCA1 is critical to Nef-dependent cholesterol trafficking, inhibition of ABCA1 would also inhibit Nef-dependent cholesterol delivery to lipid rafts.

First, we used functional inhibitors of cholesterol trafficking, blocking lipid transfer (BLT) compounds. BLT compounds inhibit ABCA1 and scavenger receptor type B1 (SR-B1)–dependent trafficking of cholesterol for efflux without affecting the abundance of the transporters (25). Two BLT compounds, BLT1 and BLT4, effectively inhibited ABCA1-dependent cholesterol efflux to apoA-I from RAW 264.7 cells (**Fig. 3A**). Consistent with our previous report showing suppression of cholesterol efflux by Nef (3), the efflux from N7 cells was about half of that from RAW 264.7 cells (Fig. 3B). Only BLT1 caused a small further inhibition of cholesterol efflux, presumably through cross-inhibition of SR-B1–dependent efflux (25). Abundance of rafts in this experiment was assessed using the cholesterol oxidase method. BLT compounds did not have a statistically significant effect on the abundance of rafts in RAW 264.7 cells (Fig. 3C). However, in N7 cells, BLT compounds significantly increased the abundance of rafts (Fig. 3D). Similar results were obtained using the CT-B binding method of lipid raft analysis (supplementary Fig. I). These findings indicate that inhibition of ABCA1 function without altering its abundance is sufficient to enhance effects of Nef.

Next, we used siRNA to knock down ABCA1 in RAW 264.7 and N7 cells. In both cell types, approximately 80% knockdown efficiency was achieved (Fig. 3E), resulting in an almost complete elimination of specific cholesterol efflux to apoA-I (not shown). When the abundance of rafts was assessed by cholesterol oxidase susceptibility, knockdown of ABCA1 caused a statistically significant increase of lipid rafts in both RAW 264.7 and N7 cells; however, the magnitude of the effect was much greater in N7 cells activated with $CdCl_2$ (Fig. 3F). When lipid raft abundance was assessed by CT-B binding, knockdown of ABCA1 did not affect abundance of rafts in RAW 264.7 cells, but it caused a statistically significant increase in raft abundance in N7 cells (Fig. 3G).

In summary, both functional inhibition of the ABCA1-dependent cholesterol trafficking pathway and knockdown of ABCA1 increased the capacity of Nef to transfer cholesterol to lipid rafts. Nef may do it directly, as suggested by Peterlin's group (8), or indirectly, for example, by interfering with normal cholesterol trafficking pathways connecting cholesterol synthesis, lipid raft formation, and efflux. Combined with our recent finding that stimulation of ABCA1 expression by LXR agonists decreases Nef-dependent cholesterol delivery to rafts (6), these results indicate that Nef does not utilize ABCA1 for cholesterol trafficking to rafts. Rather, Nef-dependent inhibition of ABCA1 may contribute to raft modulation.

Nef reduces ABCA1 stability and promotes its relocalization away from the cell surface

To better understand the Nef-dependent inhibition of ABCA1, we next analyzed the effect of Nef on catabolism and intracellular distribution of ABCA1 in macrophages. To assess the rate of catabolism of ABCA1, cells were treated with LXR agonist TO-901317 for 24 h to maximally stimulate expression of ABCA1 (26). TO-901317 was then withdrawn, effectively halting ABCA1 production, and abundance of ABCA1 was followed for another 24 h in the presence or absence of apoA-I. Results of this experiment are shown in **Fig. 4A**. In the presence of apoA-I, the abundance of ABCA1 in RAW 264.7 cells did not change after a 24 h incubation, even when ABCA1 transcription was effectively stopped by withdrawal of TO-901317 (lane 2 versus 1); however, ABCA1 abundance decreased by approximately 40% in the absence of apoA-I (lane 3 versus 1). In N7 cells, the abundance of ABCA1 decreased by 60% in the presence of apoA-I (lane 5 versus 4) and by 90% in the absence of apoA-I (lane 6 versus 4). These differences were not due to differences in *ABCA1* expression,

activated RAW 264.7 and N7 cells, untransfected (control) or transfected with scrambled siRNA ($siRNA^{C}$) or ABCA1 siRNA ($siRNA^{ABCA1}$). Abundance of GAPDH was used as loading control. F: Cells were treated with cholesterol oxidase for 3 h on ice, and oxidation of plasma membrane cholesterol was assessed as described in *Materials and Methods*. Mean ± SEM of quadruplicate determinations. $^{*}P < 0.05$ (versus cells treated with $siRNA^{C}$); $^{\#}P < 0.05$ (versus cells treated with $CdCl_2 + siRNA^{C}$). G: Cells were treated with FITC-labeled cholera toxin (CT-B). Binding of CT to GM1 (a marker of rafts) was analyzed by flow cytometry. Mean ± SEM of quadruplicate determinations. $^{*}P < 0.05$ (versus $siRNA^{C}$).

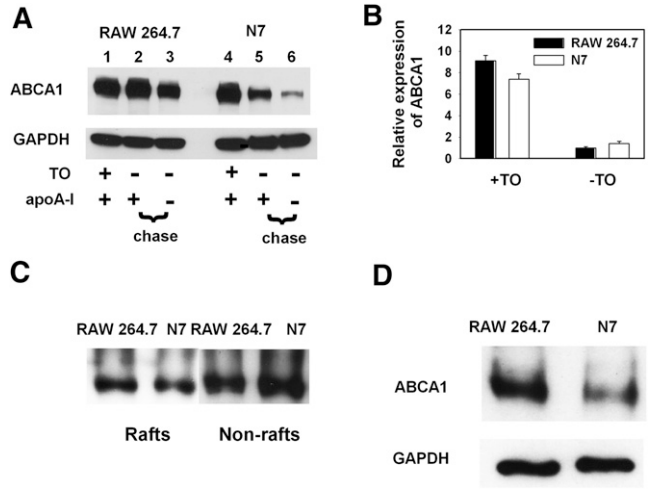

Fig. 4. Effect of Nef on abundance and cellular localization of ABCA1 in macrophages. A: Western blot showing abundance of ABCA1 in cell lysates of RAW 264.7 and N7 cells after activation of ABCA1 transcription with TO-901317 (0.5 μM), followed by withdrawal of TO-901317 and incubation for 24 h in the presence or absence of apoA-I (20 μg/ml). B: ABCA1 expression in RAW 264.7 and N7 cells stimulated or not with LXR agonist TO-901317 was analyzed by real-time RT-PCR and is presented in relative units. C: Western blot showing abundance of ABCA1 in raft versus nonraft fractions of plasma membrane in RAW 264.7 and N7 cells. Fractionation procedure is described in *Materials and Methods*. D: Analysis of surface ABCA1 by biotinylation (see *Materials and Methods* for details). GAPDH is shown as loading control.

as the abundance of *ABCA1* mRNA was not affected by Nef (Fig. 4B). Thus, Nef may increase degradation of ABCA1.

We assumed that the impairment of ABCA1 functionality and turnover by Nef may be related to changes in the subcellular localization of ABCA1. We first hypothesized that, analogous to its effect on cholesterol distribution, Nef may also facilitate ABCA1 transfer to rafts, as Nef is known to transfer a number of proteins to lipid rafts (27, 28). Such redistribution of ABCA1 from its usual nonraft location (29) may cause its dysfunction and instability. To test this hypothesis, we isolated raft and nonraft fractions of the plasma membrane and analyzed them for ABCA1. The abundance of ABCA1 in the raft fraction of N7 cells was 27% lower and in the nonraft fraction was 38% higher than that in RAW 264.7 cells (Fig. 4C). Thus, Nef did not increase the abundance of ABCA1 in rafts. Further, we assessed the accessibility of ABCA1 to biotinylation, which shows the level of ABCA1 exposure on the cell surface. The abundance of biotinylated ABCA1 in N7 cells was approximately three times lower than that in RAW 264.7 cells (Fig. 4D), despite similar levels of total ABCA1 (Fig. 4A). Therefore, we conclude that ABCA1 in Nef-expressing cells is not relocalized to the raft fraction but becomes less exposed at the cell surface, providing a possible explanation for impaired functionality and/or increased turnover of ABCA1.

Nef induces degradation of ABCA1 in lysosomes

To further investigate the interaction of Nef and ABCA1, we employed another model, HeLa cells stably transfected with ABCA1-GFP. We previously demonstrated that ABCA1-GFP in this model functions effectively in promoting cholesterol efflux to apoA-I (15, 16). This model offers the advantage of fluorescently tagged ABCA1 expression, which allows for easy tracking of ABCA1 trafficking and localization. Furthermore, ABCA1 in these cells is under control of the CMV promoter, excluding any transcriptional effects of Nef.

To assess the effect of Nef on ABCA1 distribution, HeLa-ABCA1 cells transiently transfected with Nef or an empty vector were treated with biotin, lysed, and passed through an anti-biotin column; both bound and unbound fractions were analyzed by Western blot. The bound fraction represents ABCA1 exposed at the cell surface, whereas the unbound fraction represents ABCA1 in a mixture of membranes, mainly intracellular, but also the inner leaflets of the plasma membrane. The overall abundance of ABCA1 in cells transfected with Nef was less than half compared with mock-transfected HeLa-ABCA1 cells. While the abundance of both cell surface and intracellular ABCA1 was decreased, the effect of Nef on intracellular ABCA1 was greater (**Fig. 5A**). Consequently, the ratio of cell surface/intracellular ABCA1 in Nef-transfected cells was 1.5-fold higher than in mock-transfected cells (Fig. 5B), despite an overall lower amount of cell surface ABCA1.

The same model, HeLa-ABCA1 cells, was used to further investigate the mechanisms of Nef-induced redistribution of ABCA1. Nef has been shown to reroute proteins such as CD4 to lysosomes for degradation (30). We hypothesized that the same mechanism may be responsible for reduction of intracellular ABCA1 by Nef, whereas ABCA1 on the plasma membrane would be less susceptible. To investigate this possibility, we examined the colocalization of ABCA1 and the lysosomal marker LAMP-1 in the presence or absence of Nef. GFP-ABCA1 was clearly visible in control cells and in cells transfected with Nef. ABCA1-GFP and LAMP-1–RFP displayed increased colocalization in the presence of Nef, suggesting Nef-mediated targeting of ABCA1 to lysosomes (Fig. 5C, D).

The increased colocalization of ABCA1 and LAMP-1 in the presence of Nef suggests that Nef may stimulate ABCA1 degradation via the lysosomal pathway. We tested this hypothesis by examining the effect of a lysosomal inhibitor, chloroquine, on Nef-mediated ABCA1 degradation. Nef- or mock-transfected HeLa-ABCA1-GFP cells were treated with chloroquine for 48 h, and abundance of ABCA1 was examined by Western blot (**Fig. 6A**, B). Inhibition of lysosomal activity prevented Nef-mediated reduction of ABCA1 protein abundance. Thus, Nef-mediated reduction of ABCA1 abundance depends, at least partially, on a lysosomal degradation pathway. This was further confirmed when the effect of chloroquine on cholesterol efflux was studied. When Nef- or mock-transfected HeLa-ABCA1 cells were treated with chloroquine, Nef-mediated inhibition of ABCA1-specific efflux was reversed (Fig. 6C).

The effect of Nef on macrophage functions

Inhibition of ABCA1 activity and increased abundance of lipid rafts in Nef-expressing cells may have significant

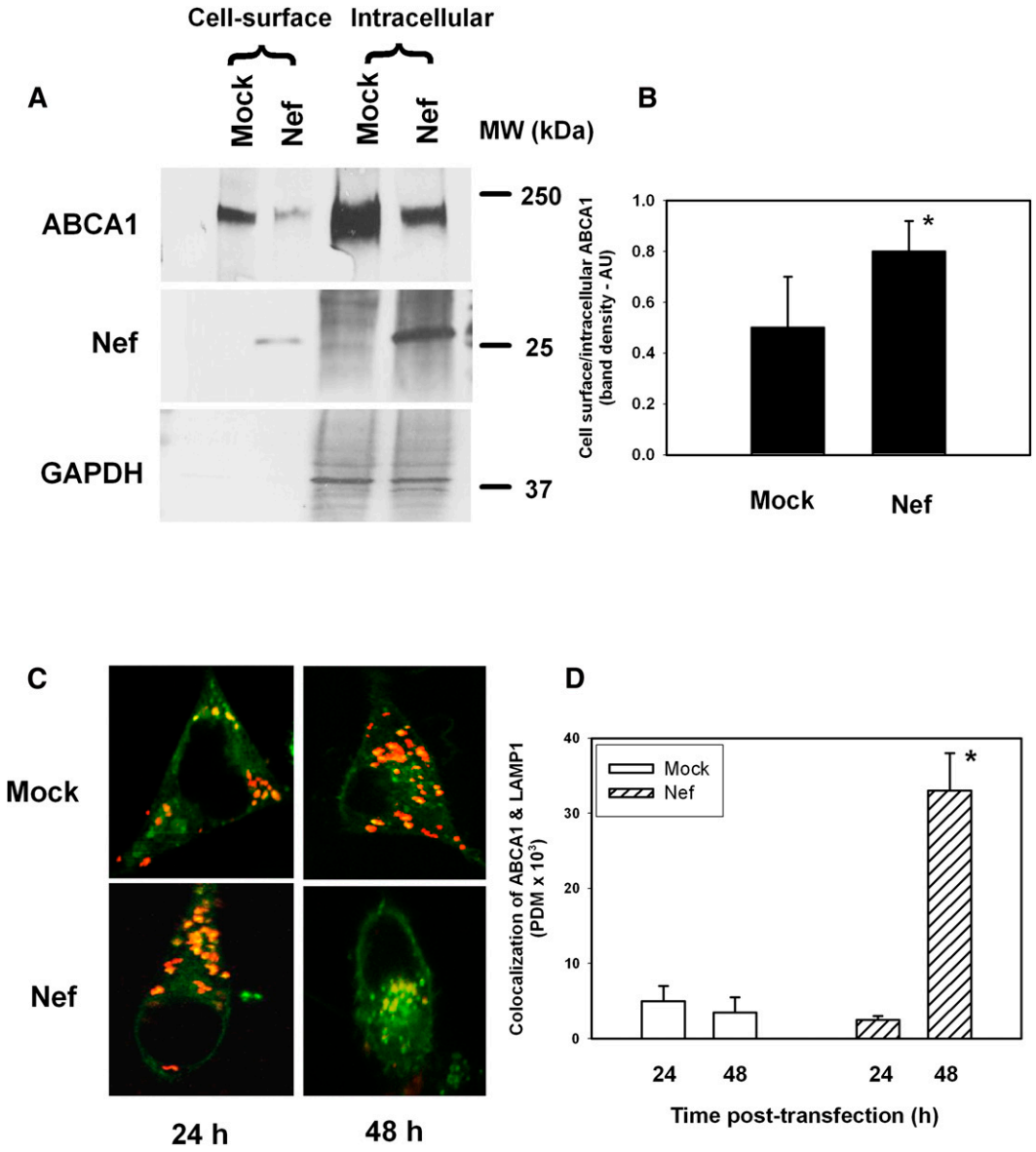

Fig. 5. Effect of Nef on abundance and cellular localization of ABCA1 in HeLa-ABCA1 cells. A: Western blot showing abundance of ABCA1 in plasma membrane and intracellular fractions in HeLa-ABCA1 cells transfected with Nef-expressing or an empty vector (mock). B: Ratio of plasma membrane to intracellular ABCA1 calculated by densitometry of Western blot data from three independent experiments. Results are presented in arbitrary units (AU) as mean ± SEM; $*P < 0.05$. C: Confocal microscopy of mock-transfected (top row) and Nef-transfected HeLa-ABCA1 cells. Green, ABCA1; orange, LAMP-1. D: Quantitation of the colocalization of ABCA1 and LAMP-1 was performed by Volocity software. $*P < 0.05$ versus mock-transfected cells.

effects on macrophage immune functions (31). To investigate this possibility, we first assessed the effect of Nef on endocytosis. Using GFP-conjugated CT-B, which binds to lipid raft–associated GM1, we found increased CT-B binding to N7 cells versus RAW 264.7 macrophages (**Fig. 7A**). This is consistent with Nef-mediated increase of lipid raft abundance. However, internalization of bound CT-B was much less efficient in N7 than in RAW 264.7 cells: whereas mean fluorescence intensity increased 5.6-fold when RAW 264.7 cells were incubated at 37°C instead of 4°C, in N7 cells, the increase was only 1.2-fold. A similar outcome was observed when another function of macrophages, phagocytosis, was analyzed using particles with pH-sensitive fluorescent dye pHrodo. Both LPS-stimulated (Fig. 7B) and unstimulated (Fig. 7C) phagocytosis was severely impaired in N7 cells compared with RAW 264.7 cells. Furthermore, treatment of N7 cells with Nef siRNA restored the level of LPS-stimulated phagocytosis in these cells to that in RAW 264.7 cells (Fig. 7B). Therefore, Nef inhibits endocytic and phagocytic functions of macrophages.

HIV-1 infectivity negatively correlates with ABCA1 expression in host cells

We previously demonstrated that pharmacological stimulation of ABCA1 expression inhibits HIV-1 infectivity by depleting viral cholesterol (6). An intriguing consequence

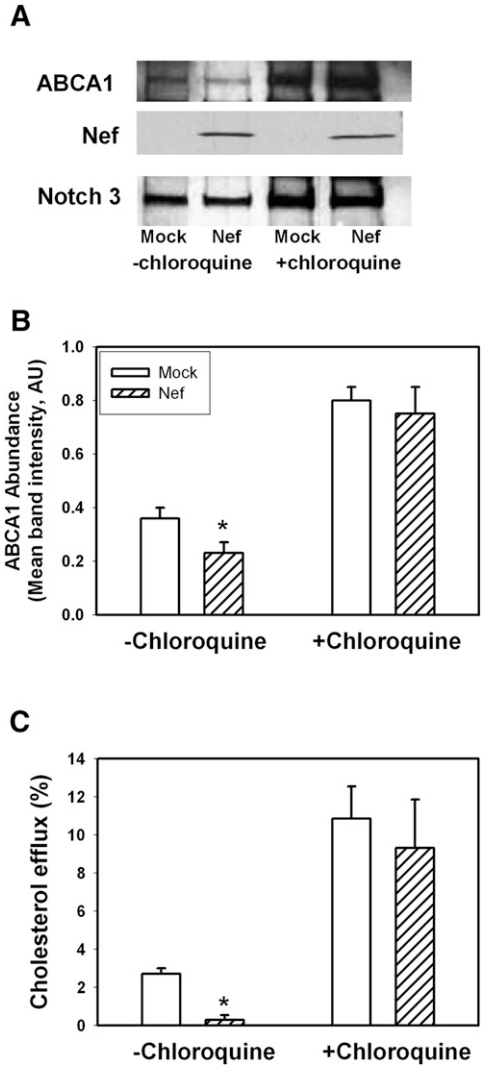

Fig. 6. Effect of chloroquine on Nef-induced downregulation of ABCA1 and cholesterol efflux. A: Western blot showing abundance of ABCA1 in HeLa-ABCA1 cells transfected with Nef or empty vector (mock) and treated or not treated with chloroquine (50 μM). B: Densitometry of the ABCA1-specific bands. Results are presented as mean ± SEM of four independent experiments similar to that shown in Fig. 4A. $*P < 0.05$. C: Cholesterol efflux to apoA-I from HeLa-ABCA1 transfected with Nef or an empty vector and treated or not treated with chloroquine (50 μM). Results are presented as mean ± SEM of three independent experiments. $*P < 0.01$.

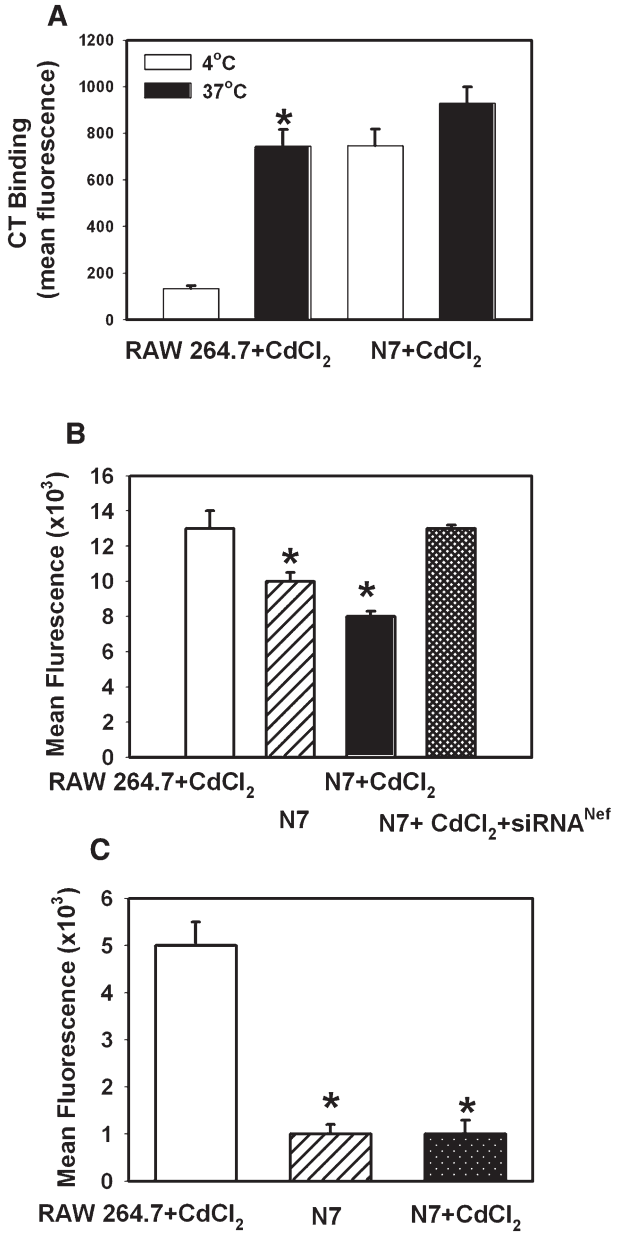

Fig. 7. Effect of Nef on macrophage functions. A: Binding (4°C) and internalization (37°C) of FITC-labeled cholera toxin (CT-B) by $CdCl_2$-treated N7 and RAW 264.7 cells. Results are presented as mean fluorescence intensity of one representative experiment out of two performed. $*P < 0.001$ (versus 4°C). B: LPS-stimulated phagocytosis in RAW 264.7 cells and N7 cells activated or not with $CdCl_2$ was assessed by measuring fluorescence of pHrodo pH-sensitive particles (Invitrogen). Results are presented as mean fluorescent intensity ± SEM of three independent experiments. $*P < 0.001$. C: Unstimulated phagocytosis in RAW 264.7 cells and N7 cells activated or not with $CdCl_2$. Results are presented as mean fluorescent intensity ± SEM of three independent experiments. $*P < 0.001$.

of this finding is that HIV infectivity may be influenced by the level of ABCA1 abundance in infected cells. To investigate this possibility, we compared HIV infectivity in two human cell types that are the primary targets of natural HIV-1 infection, macrophages and T lymphocytes. Monocyte-derived macrophages (MDM) have high abundance of ABCA1, which was readily activated by LXR agonist TO-901317 (**Fig. 8A**). Peripheral blood leukocytes (PBL) have undetectable levels of ABCA1 under basal conditions, but ABCA1 expression in these cells can be upregulated with the LXR agonist. Consistent with our expectations, infectivity of HIV-1 produced by "high ABCA1" cell type MDM was about 30% of that of virus produced by "low ABCA1" cell type PBL (Fig. 8B). This difference was eliminated when ABCA1 in MDM was suppressed by siRNA (Fig. 8B). Thus, high expression of ABCA1 in host cells is detrimental for HIV-1 infectivity.

DISCUSSION

In this study, we investigated the interaction between viral and host pathways of cholesterol trafficking: Nef-mediated transfer of cholesterol to lipid rafts and ABCA1-dependent cholesterol efflux. Both pathways transfer cholesterol from intracellular compartments to the plasma membrane, but the eventual fate of cholesterol is different: the Nef pathway utilizes cholesterol for formation of lipid rafts required for viral assembly, whereas ABCA1 facilitates cholesterol release from cells to an extracellular acceptor. The two pathways intrinsically oppose each other, as the Nef-dependent pathway results in formation of rafts and the ABCA1-dependent pathway leads to disruption of rafts (32, 33). Thus, it would be beneficial for the virus to either subvert or suppress the ABCA1-dependent cholesterol trafficking. We considered two possible interactions between the viral and host pathways of cholesterol trafficking. One possibility was that HIV hijacks the cellular ABCA1-dependent pathway, diverting the flow of cholesterol away from nonraft sites suitable for efflux (29) and to lipid rafts. The hijack strategy is often used by microorganisms, especially viruses, to compensate for limitations in the size of their genome (34). Another possibility was that HIV suppresses ABCA1 functionality to preserve cholesterol needed by the virus.

To distinguish between these two possibilities, we investigated whether inhibition of the ABCA1-dependent pathway would affect Nef-dependent cholesterol trafficking to rafts. We expected that if ABCA1 is hijacked by the Nef-dependent pathway, functional and physical inhibition of ABCA1 would inhibit Nef-mediated cholesterol delivery to rafts. Contrary to these expectations, we observed a stimulation of Nef-dependent trafficking of cholesterol to rafts after reducing ABCA1 levels or after inhibiting ABCA1-dependent cholesterol trafficking. Combined with the observation that pharmacological stimulation of ABCA1 expression inhibits HIV infectivity (6), these findings suggest that HIV does not utilize ABCA1 to transfer cholesterol to rafts but, rather, that the two pathways compete with each other.

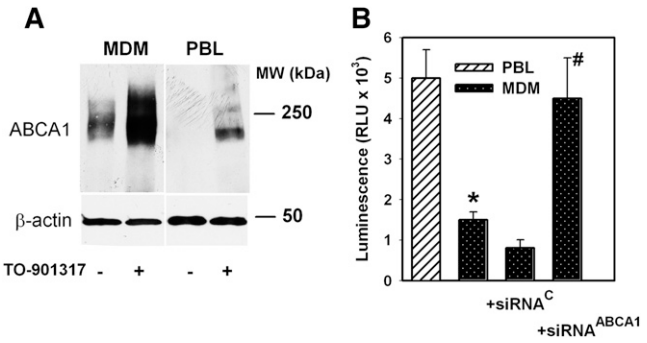

Fig. 8. Analysis of HIV-1 infectivity. A: Western blot showing ABCA1 abundance in human monocyte-derived macrophages (MDM) and peripheral blood leukocytes (PBL) with or without activation with LXR agonist TO-901317 (1 μM). B: HIV-1 ADA collected from MDM and PBL was normalized by p24 content, and viral infectivity was tested on TZM-bl indicator cells by measuring luciferase activity. MDM were transfected with ABCA1-directed or control siRNA (see *Materials and Methods*). Results of one representative experiment out of three performed with cells from different donors are presented in relative luminescence units (RLU) as mean ± SEM of triplicate determinations. $^{*}P < 0.01$ (versus PBL); $^{\#}P < 0.01$ (versus siRNA^{C}).

We used two cellular models to investigate the mechanisms of ABCA1 inhibition by Nef: RAW 264.7 macrophages stably transfected with Nef and HeLa-ABCA1 cells transiently transfected with Nef. In both cell types, the amount of ABCA1 on the surface of the cells was dramatically reduced by Nef, which may be one mechanism of cholesterol efflux inhibition in Nef-expressing cells. Surprisingly, in LXR agonist–stimulated macrophages stably transfected with Nef, the total abundance of ABCA1 was not reduced, an observation in conflict with the findings in a HeLa cell model and in other cells transiently transfected with Nef (3, 35). However, when LXR agonist was removed and cells were incubated in serum-free medium (to remove protection of ABCA1 from degradation by apoA-I), the amount of ABCA1 in Nef-expressing macrophages rapidly declined below its level in control cells under the same conditions. This finding suggests that the apparent redistribution of ABCA1 may be associated with its enhanced degradation. Experiments in HeLa cells cotransfected with ABCA1 and Nef indicated that this degradation is likely to take place in lysosomes.

Given that increased abundance of lipid rafts is considered pro-inflammatory, whereas functional ABCA1 is considered anti-inflammatory (4) and that lipid rafts function to promote endocytosis and phagocytosis in macrophages (36), we expected to see an increase of raft-associated functional activities in Nef-expressing cells. Surprisingly, despite increased binding of CT-B to Nef-expressing or HIV-infected macrophages, endocytosis and phagocytosis in these cells were impaired. This finding is in conflict with a previous report by Kedzierska et al. (37) who found that Nef does not inhibit phagocytosis of mycobacterium avium complex (MAC) by monocytes. However, that study did not identify any increase in phagocytosis by Nef, suggesting that either phagocytosis in that model did not depend on lipid rafts or that phagocytosis stimulating and inhibiting effects of Nef nullified each other. The mechanism of endocytosis and phagocytosis impairment in our model is unclear, but it is Nef-mediated and may be related to the effects of Nef on trafficking of membrane-bound proteins to and from rafts (38).

Our finding that infectivity of HIV-1 virions produced by lymphocytes is much higher than infectivity of virions released by MDM and that this difference is eliminated when ABCA1 expression in MDM is knocked down by siRNA is consistent with our previous report that ABCA1 inhibits HIV-1 infectivity via decreasing cholesterol in lipid rafts and thus limiting cholesterol incorporated into nascent HIV virions (6). However, this is the first demonstration that such activity may have implications for HIV-1 replication in natural target cells. Higher infectivity of virions produced from cells with low ABCA1 expression, such as nonactivated T lymphocytes or undifferentiated monocytes,

may partially compensate for lower virus production by these cells.

Taken together, results of this study demonstrate that Nef triggers a relocalization of ABCA1, making it less accessible at the cell surface and more susceptible to degradation, resulting in an inhibition of cholesterol efflux and increased abundance of lipid rafts. We propose the following model of this phenomenon (**Fig. 9**). Under normal circumstances, ABCA1 recirculates between plasma membrane, where it is located in nonraft compartments, and intracellular compartments, mainly early endosomes, late endocytic vesicles, and lysosomes (16) (Fig. 9A). Nef may affect recirculation by directly or indirectly preventing ABCA1 from returning to the cell surface, instead redirecting it to lysosomes. Reduced ABCA1 abundance on plasma membrane promotes formation of more rafts. On the other hand, Nef by itself may stimulate formation of rafts, reducing abundance of nonraft compartment suitable for ABCA1, shifting a balance between plasma membrane and intracellular ABCA1 toward the latter. However, ABCA1 does not accumulate in the intracellular compartments; instead, with possible assistance of Nef, the flow of ABCA1 shifts toward lysosomes, causing rapid degradation of ABCA1 (Fig. 9B). Preventing degradation of ABCA1 in the lysosomes apparently shifts the balance back toward the plasma membrane. The result of this activity is 2-fold: it promotes viral assembly and infectivity, and it affects functional capacity of targeted cells, in particular macrophages. This study implicates ABCA1 as a key molecule targeted by HIV to facilitate viral propagation while at the same time disabling cellular defenses, and it underscores the role of ABCA1 as an innate anti-HIV factor. The mechanisms described in this study might not be unique for HIV and might be used by other microorganisms whose life cycles depend upon raft cholesterol to achieve the same outcome.

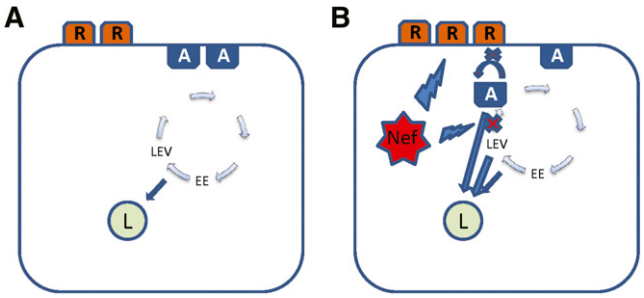

Fig. 9. Proposed model of the effect of Nef on ABCA1 abundance. A: Under normal circumstances, ABCA1 (A) recirculates between plasma membrane, where it is located in nonraft compartments and an intracellular compartment of mainly early endosomes (EE), late endocytic vesicles, (LEV) and lysosomes (L). R, raft. B: Nef may affect recirculation by preventing ABCA1 from returning to the cell surface, instead redirecting it to lysosomes; reduced ABCA1 abundance on plasma membrane leads to the formation of more rafts. Nef may also stimulate formation of rafts by reducing the abundance of nonraft compartments suitable for ABCA1, thus shifting a balance between plasma membrane and intracellular ABCA1 toward the latter. ABCA1 that is unable to reach plasma membrane is also redirected to lysosomes, possibly with the assistance of Nef.

The TZM-bl reagent was obtained from Dr. John C. Kappes, Dr. Xiaoyun Wu, and Tranzyme, Inc., through the AIDS Research and Reference Reagent Program, Division of AIDS, National Institute of Allergy and Infectious Diseases, National Institutes of Health. The N7 mouse macrophage cell line was obtained from the Centre for AIDS Reagents, National Institute for Biological Standards and Control, United Kingdom.

REFERENCES

1. Bukrinsky, M., and D. Sviridov. 2006. Human immunodeficiency virus infection and macrophage cholesterol metabolism. *J. Leukoc. Biol.* **80:** 1044–1051.
2. Rose, H., J. Hoy, I. Woolley, U. Tchoua, M. Bukrinsky, A. Dart, and D. Sviridov. 2008. HIV infection and high density lipoprotein metabolism. *Atherosclerosis.* **199:** 79–86.
3. Mujawar, Z., H. Rose, M. P. Morrow, T. Pushkarsky, L. Dubrovsky, N. Mukhamedova, Y. Fu, A. Dart, J. M. Orenstein, Y. V. Bobryshev, et al. 2006. Human immunodeficiency virus impairs reverse cholesterol transport from macrophages. *PLoS Biol.* **4:** e365.
4. Fitzgerald, M. L., Z. Mujawar, and N. Tamehiro. 2010. ABC transporters, atherosclerosis and inflammation. *Atherosclerosis.* **211:** 361–370.
5. Asztalos, B. F., Z. Mujawar, M. P. Morrow, A. Grant, T. Pushkarsky, C. Wanke, R. Shannon, M. Geyer, F. Kirchhoff, D. Sviridov, et al. 2010. Circulating Nef induces dyslipidemia in simian immunodeficiency virus-infected macaques by suppressing cholesterol efflux. *J. Infect. Dis.* **202:** 614–623.
6. Morrow, M. P., A. Grant, Z. Mujawar, L. Dubrovsky, T. Pushkarsky, Y. Kiselyeva, L. Jennelle, N. Mukhamedova, A. T. Remaley, F. Kashanchi, et al. 2010. Stimulation of the liver X receptor pathway inhibits HIV-1 replication via induction of ATP-binding cassette transporter A1. *Mol. Pharmacol.* **78:** 215–225.
7. Arora, V. K., B. L. Fredericksen, and J. V. Garcia. 2002. Nef: agent of cell subversion. *Microbes Infect.* **4:** 189–199.
8. Zheng, Y. H., A. Plemenitas, C. J. Fielding, and B. M. Peterlin. 2003. Nef increases the synthesis of and transports cholesterol to lipid rafts and HIV-1 progeny virions. *Proc. Natl. Acad. Sci. USA.* **100:** 8460–8465.
9. van't Wout, A. B., J. V. Swain, M. Schindler, U. Rao, M. S. Pathmajeyan, J. I. Mullins, and F. Kirchhoff. 2005. Nef induces multiple genes involved in cholesterol synthesis and uptake in human immunodeficiency virus type 1-infected T cells. *J. Virol.* **79:** 10053–10058.
10. Zheng, Y. H., A. Plemenitas, T. Linnemann, O. T. Fackler, and B. M. Peterlin. 2001. Nef increases infectivity of HIV via lipid rafts. *Curr. Biol.* **11:** 875–879.
11. Giese, S. I., I. Woerz, S. Homann, N. Tibroni, M. Geyer, and O. T. Fackler. 2006. Specific and distinct determinants mediate membrane binding and lipid raft incorporation of HIV-1(SF2) Nef. *Virology.* **355:** 175–191.
12. Gerlach, H., V. Laumann, S. Martens, C. F. Becker, R. S. Goody, and M. Geyer. 2010. HIV-1 Nef membrane association depends on charge, curvature, composition and sequence. *Nat. Chem. Biol.* **6:** 46–53.
13. Brügger, B., E. Krautkramer, N. Tibroni, C. E. Munte, S. Rauch, I. Leibrecht, B. Glass, S. Breuer, M. Geyer, H. G. Kräusslich, et al. 2007. Human immunodeficiency virus type 1 Nef protein modulates the lipid composition of virions and host cell membrane microdomains. *Retrovirology.* **4:** 70.
14. Cooke, S. J., K. Coates, C. H. Barton, T. E. Biggs, S. J. Barrett, A. Cochrane, K. Oliver, J. A. McKeating, M. P. Harris, and D. A. Mann. 1997. Regulated expression vectors demonstrate cell-type-specific sensitivity to human immunodeficiency virus type 1 Nef-induced cytostasis. *J. Gen. Virol.* **78:** 381–392.
15. Mukhamedova, N., Y. Fu, M. Bukrinsky, A. T. Remaley, and D. Sviridov. 2007. The role of different regions of ATP-binding cassette transporter A1 in cholesterol efflux. *Biochemistry.* **46:** 9388–9398.
16. Neufeld, E. B., A. T. Remaley, S. J. Demosky, J. A. Stonik, A. M. Cooney, M. Comly, N. K. Dwyer, M. Zhang, J. Blanchette-Mackie, S.

Santamarina-Fojo, et al. 2001. Cellular localization and trafficking of the human ABCA1 transporter. *J. Biol. Chem.* **276:** 27584–27590.
17. Brace, R. J., B. Sorrenson, D. Sviridov, and S. P. A. McCormick. 2010. A gel-based method for purification of apolipoprotein A-I from small volumes of plasma. *J. Lipid Res.* **51:** 3370–3376.
18. Wei, X., J. M. Decker, H. Liu, Z. Zhang, R. B. Arani, J. M. Kilby, M. S. Saag, X. Wu, G. M. Shaw, and J. C. Kappes. 2002. Emergence of resistant human immunodeficiency virus type 1 in patients receiving fusion inhibitor (T-20) monotherapy. *Antimicrob. Agents Chemother.* **46:** 1896–1905.
19. Sviridov, D., N. Fidge, G. Beaumier-Gallon, and C. Fielding. 2001. Apolipoprotein A-I stimulates the transport of intracellular cholesterol to cell-surface cholesterol-rich domains (caveolae). *Biochem. J.* **358:** 79–86.
20. Mukhamedova, N., G. Escher, W. D'Souza, U. Tchoua, A. Grant, Z. Krozowski, M. Bukrinsky, and D. Sviridov. 2008. Enhancing apolipoprotein A-I-dependent cholesterol efflux elevates cholesterol export from macrophages in vivo. *J. Lipid Res.* **49:** 2312–2322.
21. Patlolla, J. M., M. V. Swamy, J. Raju, and C. V. Rao. 2004. Overexpression of caveolin-1 in experimental colon adenocarcinomas and human colon cancer cell lines. *Oncol. Rep.* **11:** 957–963.
22. Le Lay, S., Q. Li, N. Proschogo, M. Rodriguez, K. Gunaratnam, S. Cartland, C. Rentero, W. Jessup, T. Mitchell, and K. Gaus. 2009. Caveolin-1-dependent and -independent membrane domains. *J. Lipid Res.* **50:** 1609–1620.
23. Gaus, K., T. Zech, and T. Harder. 2006. Visualizing membrane microdomains by Laurdan 2-photon microscopy. *Mol. Membr. Biol.* **23:** 41–48.
24. Owen, D. M., C. Rentero, A. Magenau, A. Abu-Siniyeh, and K. Gaus. 2011. Quantitative imaging of membrane lipid order in cells and organisms. *Nat. Protoc.* **7:** 24–35.
25. Nieland, T. J. F., A. Chroni, M. L. Fitzgerald, Z. Maliga, V. I. Zannis, T. Kirchhausen, and M. Krieger. 2004. Cross-inhibition of SR-BI- and ABCA1-mediated cholesterol transport by the small molecules BLT-4 and glyburide. *J. Lipid Res.* **45:** 1256–1265.
26. Rigamonti, E., G. Chinetti-Gbaguidi, and B. Staels. 2008. Regulation of macrophage functions by PPAR-{alpha}, PPAR-{gamma}, and LXRs in mice and men. *Arterioscler. Thromb. Vasc. Biol.* **28:** 1050–1059.
27. Rauch, S., K. Pulkkinen, K. Saksela, and O. T. Fackler. 2008. Human immunodeficiency virus type 1 Nef recruits the guanine exchange factor Vav1 via an unexpected interface into plasma membrane microdomains for association with p21-activated kinase 2 activity. *J. Virol.* **82:** 2918–2929.
28. Djordjevic, J. T., S. D. Schibeci, G. J. Stewart, and P. Williamson. 2004. HIV type 1 Nef increases the association of T cell receptor (TCR)-signaling molecules with T cell rafts and promotes activation-induced raft fusion. *AIDS Res. Hum. Retroviruses.* **20:** 547–555.
29. Mendez, A. J., G. Lin, D. P. Wade, R. M. Lawn, and J. F. Oram. 2001. Membrane lipid domains distinct from cholesterol/sphingomyelin-rich rafts are involved in the ABCA1-mediated lipid secretory pathway. *J. Biol. Chem.* **276:** 3158–3166.
30. daSilva, L. L., R. Sougrat, P. V. Burgos, K. Janvier, R. Mattera, and J. S. Bonifacino. 2009. Human immunodeficiency virus type 1 Nef protein targets CD4 to the multivesicular body pathway. *J. Virol.* **83:** 6578–6590.
31. Yvan-Charvet, L., N. Wang, and A. R. Tall. 2010. Role of HDL, ABCA1, and ABCG1 transporters in cholesterol efflux and immune responses. *Arterioscler. Thromb. Vasc. Biol.* **30:** 139–143.
32. Koseki, M., K. Hirano, D. Masuda, C. Ikegami, M. Tanaka, A. Ota, J. C. Sandoval, Y. Nakagawa-Toyama, S. B. Sato, T. Kobayashi, et al. 2007. Increased lipid rafts and accelerated lipopolysaccharide-induced tumor necrosis factor-{alpha} secretion in Abca1-deficient macrophages. *J. Lipid Res.* **48:** 299–306.
33. Landry, Y. D., M. Denis, S. Nandi, S. Bell, A. M. Vaughan, and X. Zha. 2006. ATP-binding cassette transporter A1 expression disrupts raft membrane microdomains through its ATPase-related functions. *J. Biol. Chem.* **281:** 36091–36101.
34. Mañes, S., G. del Real, and C. Martínez-A. 2003. Pathogens: raft hijackers. *Nat. Rev. Immunol.* **3:** 557–568.
35. Mujawar, Z., N. Tamehiro, A. Grant, D. Sviridov, M. Bukrinsky, and M. L. Fitzgerald. 2010. Mutation of the ATP cassette binding transporter A1 (ABCA1) C-terminus disrupts HIV-1 Nef binding but does not block the Nef enhancement of ABCA1 protein degradation. *Biochemistry.* **49:** 8338–8349.
36. Nagao, G., K. Ishii, K. Hirota, K. Makino, and H. Terada. 2010. Role of lipid rafts in phagocytic uptake of polystyrene latex microspheres by macrophages. *Anticancer Res.* **30:** 3167–3176.
37. Kedzierska, K., J. Mak, A. Jaworowski, A. Greenway, A. Violo, H. T. Chan, J. Hocking, D. Purcell, J. S. Sullivan, J. Mills, et al. 2001. Nef-deleted HIV-1 inhibits phagocytosis by monocyte-derived macrophages in vitro but not by peripheral blood monocytes in vivo. *AIDS.* **15:** 945–955.
38. Roeth, J. F., and K. L. Collins. 2006. Human immunodeficiency virus type 1 Nef: adapting to intracellular trafficking pathways. *Microbiol. Mol. Biol. Rev.* **70:** 548–563.